J|A|C|S ARTICLES

Published on Web 07/01/2009

Electron Ionization Dissociation of Singly and Multiply Charged Peptides

Y. M. Eva Fung, Christopher M. Adams, and Roman A. Zubarev*

Division of Molecular Biometry, Department of Medicinal Biochemistry and Biophysics, Karolinska Institutet, SE-17 177 Stockholm, Sweden

Received November 19, 2008; E-mail: Roman.Zubarev@ki.se

Abstract: A new tandem mass spectrometry technique, electron ionization dissociation (EID), employs irradiation of trapped cations $[M + nH]^{n+}$ ($n \geq 1$) by fast electrons with energy at least 10 eV higher than the ionization threshold of the cations. Such irradiation causes simultaneous ionization and electronic excitation of the irradiated species, which is equivalent of double-ionization to $[M + nH]^{(n+2)+}$ followed by electron capture to form electronically excited $[M + nH]^{(n+1)+\bullet *}$ ions. Subsequent fragmentation of the latter species gives both side-chain losses and backbone fragmentation. Theoretical efficiency of such fragmentation calculated as a ratio of the fragment ion current and the precursor ion depletion can reach $(n+1)/n$, that is, can exceed 100%. EID often leads to backbone $N-C_\alpha$ bond cleavage, giving *c*-/*z*-type fragments. C−C bond cleavage, giving preferentially *a*-/*x*-type fragments, is also observed. EID could be used in bottom-up proteomics for both electrospray and matrix-assisted laser desorption ionization (MALDI) -produced ions. The energy incorporated into the precursor ion in a single interaction with electrons can exceed 10 eV, which makes EID suitable for top-down analysis of folded gas-phase protein conformations.

Introduction

In characterization of the performance of an analytical technique, two factors are usually considered: the efficiency of the technique and the quantity of analytical information it can provide. Electron capture dissociation (ECD)[1] is a technique which, together with the fundamentally similar electron transfer dissociation (ETD),[2] gained popularity in recent years. ECD/ETD is mostly used for localization of posttranslational modifications (PTMs),[3−6] differentiation of Ile/Leu (Xle) residues,[7] de novo sequencing,[8,9] and conformational analysis of gas-phase peptides/proteins.[10−12] For large molecules in high charge states, ECD performs excellently in terms of both the efficiency (>80% has been reported for multiply charged ions)[9] and the quantity of analytical information that it provides. However, the efficiency of ECD for dications is known to be relatively low when compared to conventional dissociation techniques collisionally activated dissociation (CAD)[13,14] and infrared multiphoton dissociation (IRMPD).[15,16] Because of the neutralization of one charge before fragmentation, the maximum theoretical efficiency of ECD for doubly charged precursors is about 37%,[17] as only one of the two complementary ECD fragments has a net charge that allows it to be detectable in a mass spectrometer. Yet even for dications ECD is analytically useful with respect to CAD/IRMPD, because it cleaves at different sites,[9] not to mention the cleavage of a different type of bond. The new sequence information in ECD arises due to the fact that fragmenting species are $(n-1)+$ radical cations as opposed to $n+$ even-electron ions in CAD/IRMPD. The presence of a radical site changes the chemistry of the fragmenting ion to such a degree that ECD and CAD become truly complementary.[9]

Yet the problem of the low efficiency for dications (which in practice is 10−17%) as well as the impossibility to apply ECD to matrix-assisted laser desorption ionization (MALDI) -produced singly charged ions is a significant analytical limitation. In the present work we introduce a new technique that is based on radical chemistry but promises high efficiency even for ions with a single charge. Theoretically, this technique can

(1) Zubarev, R. A.; Kelleher, N. L.; McLafferty, F. W. *J. Am. Chem. Soc.* **1998**, *120*, 3265–3266.
(2) Syka, J. E. P.; Coon, J. J.; Schroeder, M. J.; Shabanowitz, J.; Hunt, D. F. *Proc. Natl. Acad. Sci. U.S.A.* **2004**, *101*, 9528–9533.
(3) Kelleher, R. L.; Zubarev, R. A.; Bush, K.; Furie, B.; Furie, B. C.; McLafferty, F. W.; Walsh, C. T. *Anal. Chem.* **1999**, *71*, 4250–4253.
(4) Mirgorodskaya, E.; Roepstorff, P.; Zubarev, R. A. *Anal. Chem.* **1999**, *71*, 4431–4436.
(5) Stensballe, A.; Jensen, O. N.; Olsen, J. V.; Haselmann, K. F.; Zubarev, R. A. *Rapid Commun. Mass Spectrom.* **2000**, *14*, 1793–1800.
(6) Shi, S. D. H.; Hemling, M. E.; Carr, S. A.; Horn, D. M.; Lindh, I.; McLafferty, F. W. *Anal. Chem.* **2001**, *73*, 19–22.
(7) Kjeldsen, F.; Haselmann, K. F.; Budnik, B. A.; Jensen, F.; Zubarev, R. A. *Chem. Phys. Lett.* **2002**, *356*, 201–206.
(8) Horn, D. M.; Zubarev, R. A.; McLafferty, F. W. *Proc. Natl. Acad. Sci. U.S.A.* **2000**, *97*, 10313–10317.
(9) Zubarev, R. A.; Horn, D. M.; Fridriksson, E. K.; Kelleher, N. L.; Kruger, N. A.; Lewis, M. A.; Carpenter, B. K.; McLafferty, F. W. *Anal. Chem.* **2000**, *72*, 563–573.
(10) Breuker, K.; Oh, H. B.; Horn, D. M.; Cerda, B. A.; McLafferty, F. W. *J. Am. Chem. Soc.* **2002**, *124*, 6407–6420.
(11) Oh, H.; Breuker, K.; Sze, S. K.; Ge, Y.; Carpenter, B. K.; McLafferty, F. W. *Proc. Natl. Acad. Sci. U.S.A.* **2002**, *99*, 15863–15868.
(12) Breuker, K.; McLafferty, F. W. *Angew. Chem., Int. Ed. Engl.* **2003**, *42*, 4900–4904.
(13) Haddon, W. F.; McLafferty, F. W. *J. Am. Chem. Soc.* **1968**, *90*, 4745–4746.
(14) Rozett, R. W.; Koski, W. S. *J. Chem. Phys.* **1968**, *49*, 2691–2695.
(15) Little, D. P.; Speir, J. P.; Senko, M. W.; O'Connor, P. B.; McLafferty, F. W. *Anal. Chem.* **1994**, *66*, 2809–2815.
(16) Price, W. D.; Schnier, P. D.; Williams, E. R. *Anal. Chem.* **1996**, *68*, 859–866.
(17) Zubarev, R. A.; Haselmann, K. F.; Budnik, B.; Kjeldsen, F.; Jensen, F. *Eur. J. Mass Spectrom.* **2002**, *8*, 337−349.

reach >100% efficiency. It is called electron ionization dissociation (EID), as it is based on the phenomenon of tandem ionization of trapped peptide cations.[18] Implementation of EID is similar to that of ECD, but the electron energy in EID is much larger. It has been known since the late 1990s that irradiation of polyatomic $[M + nH]^{n+}$ ions by electrons with kinetic energy higher than their ionization threshold causes ionization of the latter species to radicals $[M + nH]^{(n+1)+\bullet}$. However, ionization per se does not cause dissociation of the formed radicals. While the ionization efficiency reaches a maximum at ≈20 eV,[19] at this energy no fragmentation occurs except for losses of small neutral groups.[18,20] In order to fragment the ionized species, additional energy has to be incorporated.

One way to impart additional energy into the oxidized radical cations $(n+1)+\bullet$ (chemically, ionization of ions amounts to their oxidation, while electron capture amounts to their reduction) is via low-energy electron capture, which can release recombination energy as high as ionization energy of the $n+$ precursors, that is, ca. 11 eV. However, the species formed as a result of electron capture will be electronically excited precursors $[M + nH]^{n+}*$ that will mostly fragment through C−C and C−N backbone cleavage. The corresponding technique is called electronic excitation dissociation, EED.[21] The efficiency of EED is even lower than in ECD because it is a two-stage process, with each step involving losses.

The alternative way to incorporate more energy in the oxidized $(n+1)+\bullet$ ions is by their electronic excitation. It can be hypothesized, based on the experience from 70 eV electron ionization of volatile organic molecules, that higher electron energies should lead to abundant fragmentation of the electronically excited radicals $[M + nH]^{(n+1)+\bullet}$. However, performing such an experiment is a difficult task. Tandem ionization is typically done in a Penning cell of a Fourier transform ion cyclotron resonance (FT ICR) mass spectrometer, which has low trapping ability in the axial direction along which the electron beam propagates. As a result, irradiation with >20 eV electrons causes significant losses in the FT ICR signal. The most likely reasons for this signal loss are both the axial excitation and magnetron expansion.

Recent advances in the FT ICR technology include introduction of the Ultra trap implemented in a 7 T linear ion trap quadrupole (LTQ) Fourier transform (FT) mass spectrometer.[22] The Ultra trap is characterized by better control over the potentials inside the trap and higher cyclotron orbit of ion excitation. Both these features are beneficial for tandem ionization, as carefully centered ion cloud undergoes lesser magnetron expansion. Indeed, it is possible to irradiate ions in the Ultra trap by up to 100 eV electron without fatal signal loss. The experiments described below showed that the character of tandem ionization mass spectra changes as the electron energy exceeds 30 eV. Besides the ionized species $[M + nH]^{(n+1)+\bullet}$ and small losses from them, backbone fragments appear. It is clear that the fragmenting species are not even-electron ions, as in EED, but radical cations as in ECD (although they are hydrogen-deficient cations and not hydrogen-abundant species as in ECD). Since backbone fragmentation occurs in $(n+1)+\bullet$ ions, the efficiency of the overall fragmentation process starting from $n+$ precursors can theoretically approach $(n+1)/n$, that is, significantly exceed 100%. In practice, such a high efficiency is difficult to demonstrate because of the inevitable signal losses during irradiation. Still, we were able to obtain >100% efficiency in certain cases, as described below. We also investigated the mechanism in EID, especially of $N-C_\alpha$ bond cleavage, and found evidence for ECD-like fragmentation.

Experimental Section

Materials and Sample Preparation. Ubiquitin was obtained from Sigma. All smaller polypeptides were synthesized in-house by solid-phase peptide synthesis via the N-α-Fmoc (Fmoc = 9-fluorenylmethoxycarbonyl) protocol.[23] A research-grade microscale ResPep peptide synthesizer (Intavis AG, Gladbach, Germany) was used to produce 5 μmol of each polypeptide. Capping (acetylation of the N-terminus) between each amino acid coupling suppressed the undesired truncated polypeptides and increased the yield of the desired product. The produced peptides were then purified by reverse-phase high-performance liquid chromatography (RP-HPLC) (HP1100, Agilent, CA) on a C18 column. For mass spectrometric (MS) analysis, polypeptides were diluted to a final concentration of ca. 10^{-6} M in a water/methanol/acetic acid (49:49:2 v/v/v) mixture.

Mass Spectrometry. A 7 T LTQ FT Ultra mass spectrometer (ThermoFisher Scientific, Bremen, Germany) equipped with a nanoelectrospray ion source (Proxeon Biosiences, Odense, Denmark) and an indirectly heated dispenser cathode (Thermo Fisher) as an electron source was used for ECD and EID experiments. Nanoflow (10−100 nL/min) ESI infusion was performed with metal-coated pulled-glass needles (Proxeon) with an electric potential of 700−1300 V between the spraying needle and the mass spectrometer inlet. Molecular ions in a desired charge state were isolated in the linear ion trap and transferred to the Penning (ICR) trap for ECD/EID experiments. An electron current of 30 μA and irradiation time of 30 ms were used in the ECD experiment. In EID experiments, both the electron irradiation time and electron energy were adjusted to optimize the condition for ionized species formation. Optimized parameters varied depending on the molecular weight and charge states of samples. All spectra were obtained in broadband detection mode with a resolution of 100 000 at m/z 400. In each experiment, a total of 20 acquisitions each containing 10 individual spectra (microscans) were averaged. External calibration provided better than 2 ppm mass accuracy for precursor ions in the MS and ECD MS/MS modes. Because of the mass shift of EID fragments caused by the disturbance of their ionic clouds by electrons (see below), EID mass spectra were recalibrated by use of the remaining precursors and the oxidized species as internal standards.

Results and Discussion

Obtaining EID. The first step toward EID is obtaining tandem ionization, that is, abundant $[M + nH]^{(n+1)+\bullet}$ ions (oxidized species), which can be observed at >20 eV electron energy. Optimization of the experimental conditions, such as electron current and duration of ion−electron interaction, Penning trap potentials, etc., for maximum abundance of these ions was critical for the observation of these species. With such optimization performed, further increase in the electron energy to ca. 30 eV resulted in the appearance of abundant neutral losses from the oxidized species $[M + nH]^{(n+1)+\bullet}$. Experimental conditions were further optimized for maximum signal from these neutral-

(18) Budnik, B. A.; Zubarev, R. A. *Chem. Phys. Lett.* **2000**, *316*, 19–23.
(19) Berkowitz, J. *Phys. Essays* **2000**, *13*, 248–255.
(20) Zubarev, R. A.; Nielsen, M. L.; Budnik, B. A. *Eur. J. Mass Spectrom.* **2000**, *6*, 235–240.
(21) Nielsen, M. L.; Budnik, B. A.; Haselmann, K. F.; Zubarev, R. A. *Int. J. Mass Spectrom.* **2003**, *226*, 181–187.
(22) Malek, R. H.; Meyer, K. J.; Seedorf, S.; Horning, S. R. (Thermo Finnigan LLC). WO, 2004, 37; US Patent 7,211,794 B2 "Mass Spectrometer".
(23) Carpino, L. A.; Han, G. Y. *J. Org. Chem.* **1972**, *37*, 3404–3409.

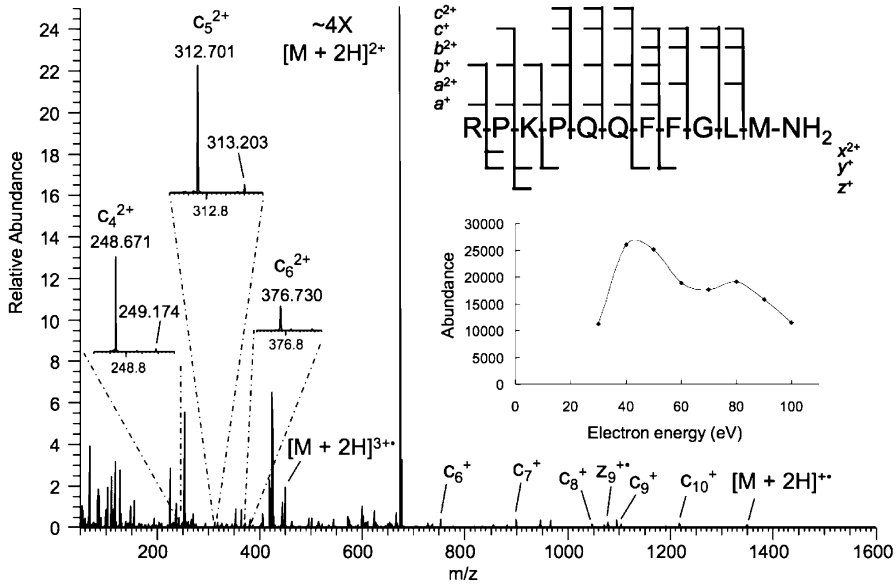

Figure 1. EID spectrum of doubly protonated substance P. (Inset) Sums of absolute abundances of c_4^{2+}, c_5^{2+}, and c_6^{2+} ions against the electron energy used.

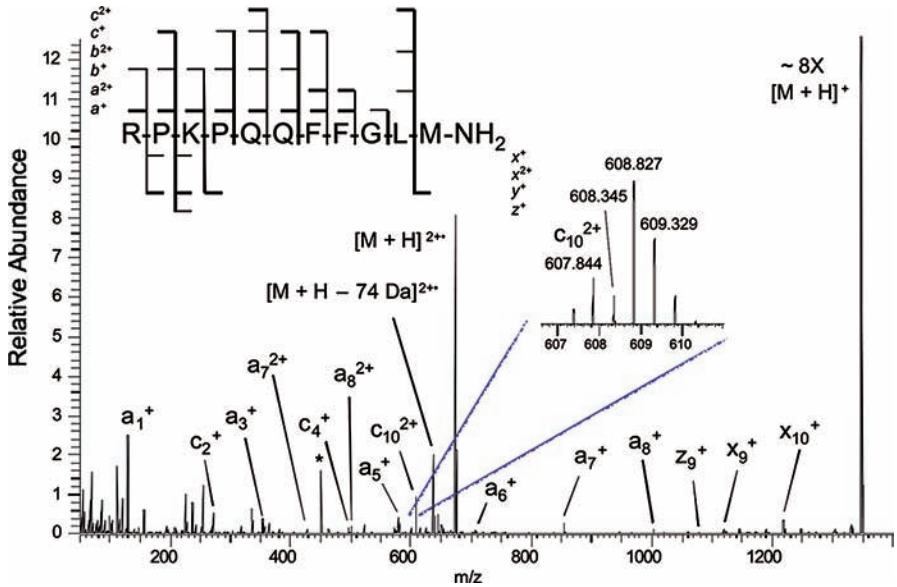

Figure 2. EID spectrum of singly protonated substance P. (Inset) Isotopic distribution of c_{10}^{2+} ions.

loss fragments. Further increase in electron energy to ca. 40 eV produced the doubly ionized species $[M + nH]^{(n+2)+}$ as well as backbone fragments. The doubly ionized species are not always easy to detect, as for 1+ and 2+ precursor ions they nearly overlap with the third and second parasitic harmonics of the precursors, respectively. Thus for the observation of double ionization the best precursors are 3+ and higher charge states.

EID of Substance P. Figure 1 demonstrates the results of an EID experiment on dications of substance P, the species widely used as a model system for testing new fragmentation techniques. The most abundant fragment ion is at *m/z* 424.908, which is the loss of 74.0193 Da from the ionized 3+ • species. This is likely to be $CH_2{=}CHSCH_3$ from Met; the theoretical mass is 74.0190 Da. Such a loss is frequently observed from ionized species. Most of the observed backbone fragments can be attributed to known processes, such as electron-impact excitation of ions from organics (EIEIO) (singly and doubly charged b and y ions) and hot electron capture dissociation (HECD) (singly and doubly charged a and x ions, singly charged w, c, and z ions). However, there are at least three doubly charged ions (c_4, c_5, and c_6) that cannot be attributed to either of these processes. The inset in Figure 1 shows the summed abundance of these three dications as a function of the electron energy. The abundance reaches a maximum at ≈40 eV and gives a smaller peak at ≈80 eV. Similar behavior was observed for other ions as well; an explanation is proposed below.

To eliminate the HECD effects, EID was performed on singly protonated substance P (Figure 2). Here, only singly charged fragments could be accounted for by the classical EIEIO mechanism, while several doubly charged fragments are observed in Figure 2, including two c-ions. Among singly charged fragments, five c- and one z-ion were detected. But the most numerous are the a-ions, of which a complete series was found, complemented by two detected x-ions. Ions of b- and y-types were also observed, albeit in relatively low abundance (a full list of substance P fragments is given in Table 1).

Table 1. Assignments of Peaks in EID Spectra of Substance P

assignment	doubly protonated precursor			singly protonated precursor		
	measured *m/z*	S/N	error (ppm)	measured *m/z*	S/N	error (ppm)
a_1^+	129.1133	373	−1.5	129.1136	656	0.8
b_1^+	157.1082	172	−1.3	157.1085	151	0.6
a_2^+	226.1661	64	−0.4	226.1664	71	0.9
c_4^{2+}	248.6713	25	−0.4			
b_2^+	254.1611	700	−0.4	254.1613	306	0.4
c_2^+	271.1877	83	0.0	271.1878	129	0.4
c_5^{2+}	312.7006	35	0.0	312.7009	9	1.0
a_3^+	354.2614	16	0.6	354.2614	44	0.6
c_6^{2+}	376.7300	5	0.3			
b_3^+	382.2563	51	0.5	382.2566	31	1.3
$[M + 2H]^{3+\bullet} - CH_2{=}CHSCH_3 - CH_2{=}C(CH_3)_2$	406.2205	79	0.3	N/A		
$[M + 2H]^{3+\bullet} - CH_2{=}CHSCH_3 - NH_3$	419.2320	284	−1.0	N/A		
$[M + 2H]^{3+\bullet} - CH_2{=}CHSCH_3$	424.9080	805	0.2	N/A		
a_7^{2+}	427.7539	65	1.2	427.7535	31	0.2
b_7^{2+}	441.7513	20	0.9			
$[M + 2H]^{3+\bullet} - NH_3$	443.9054	150	0.0	N/A		
$[M + 2H]^{3+\bullet}$	449.5811	237	0.4	N/A		
a_4^+	451.3140	11	0.0	451.3142	31	0.4
y_4^+	466.2496	7	0.6			
b_4^+	479.3099	9	2.1	479.3093	15	0.8
c_4^+	496.3358	52	0.8	496.3356	35	0.4
a_8^{2+}	501.2880	55	0.8	501.2879	46	0.6
b_8^{2+}	515.2853	39	0.4			
b_9^{2+}	543.7963	49	0.9			
a_5^+	579.3721	6	−0.7	579.3729	31	0.7
a_{10}^{2+}	586.3394	9	−1.7	586.3419	12	2.6
b_{10}^{2+}	600.3374	122	−0.7	600.3382	11	0.7
b_5^+	607.3676	28	0.2	607.3680	22	0.8
c_{10}^{2+}				607.8440	207	1.2
x_{10}^{2+}	609.8148	37	−0.2			
y_5^+	613.3174	5	−0.7			
c_5^+	624.3944	95	0.6	624.3944	35	0.6
$[M + H]^{2+\bullet} - CH_2{=}CHSCH_3$	N/A			636.8582	454	0.0
$[M + H]^{2+\bullet} - {}^{\bullet}CH_2SCH_3$	N/A			643.3622	111	0.2
$[M + H]^{2+\bullet} - {}^{\bullet}CH_2(O)NH_2$	N/A			644.8529	103	0.2
$[M + 2H]^{2+}$	674.3715	11 876	0.3	N/A		
$[M + H]^{2+\bullet}$	N/A			673.8626[a]	507	7.1
a_6^+	707.4282	6	−4.1	707.4317	19	0.8
b_6^+	735.4276	17	2.2	735.4267	7	1.0
c_6^+	752.4538	44	1.6	752.4526	11	0.0
a_7^+	854.5015	13	2.3	854.4998	63	0.4
b_7^+	882.4966	11	2.5			
c_7^+	899.5238	49	3.1	899.5198	3	−1.3
y_8^+	966.4880	41	0.3	966.4855	6	−2.3
a_8^+				1001.5684	28	0.5
c_8^+	1046.5914	21	1.9			
$z_9^{+\bullet}$	1078.5631	33	−0.7	1078.5613	7	−2.4
y_9^+	1094.5852	42	2.4	1094.5826	2	0.0
c_9^+	1103.6124	17	1.4			
x_9^+				1121.5642	17	−4.9
y_{10}^+	1191.6342	6	−1.0	1191.6339	25	−1.3
c_{10}^+	1216.7008	25	4.8			
x_{10}^+				1218.6219	77	−0.5
$[M + 2H]^{+\bullet}$	1348.7453	15	2.0	N/A		

[a] Peaks overlap with harmonics of precursor ions.

By far the most abundant EID products in both Figures 1 and 2 are the oxidized (charge-increased) species. Less abundant are the neutral losses from these species, followed by backbone cleavages. Backbone cleavages appear only above electron energies at which the abundance of the oxidized species reaches maximum, consistent with the latter species being the intermediates for the backbone-cleavage fragments.

Side-Chain Losses from $[M + nH]^{(n+1)+\bullet}$. Small side-chain losses are characteristic features of the fragmentation mechanism. In CAD, abundant losses of molecules (H_2O and NH_3) are approximately equally common, while ammonia losses from the reduced species in ECD are orders of magnitude more abundant than water losses. To probe the similarity and differences between ECD (electron energy 0−4 eV; irradiation time 30 ms) and EID (electron energy ca. 50 eV; irradiation time 20 ms), we have compared small losses from the reduced and oxidized species, respectively, for the same charge state and the same molecule, peptide DSHAKRHHGYKRKFHEKHHSHRGY (Figure 3). To obtain the same charge state, 7+ precursor ions were used in ECD and 5+ precursors in EID. The so-called $[M^{\bullet} - X]$ regions are compared in Figure 4. Even at the level of nominal mass they show dramatic differences in both the composition and the abundance of the losses. It is important to note that, while the charge states of the reduced and oxidized species in Figures 3 and 4 are the same, and they both are radicals, the chemical natures of these species are very

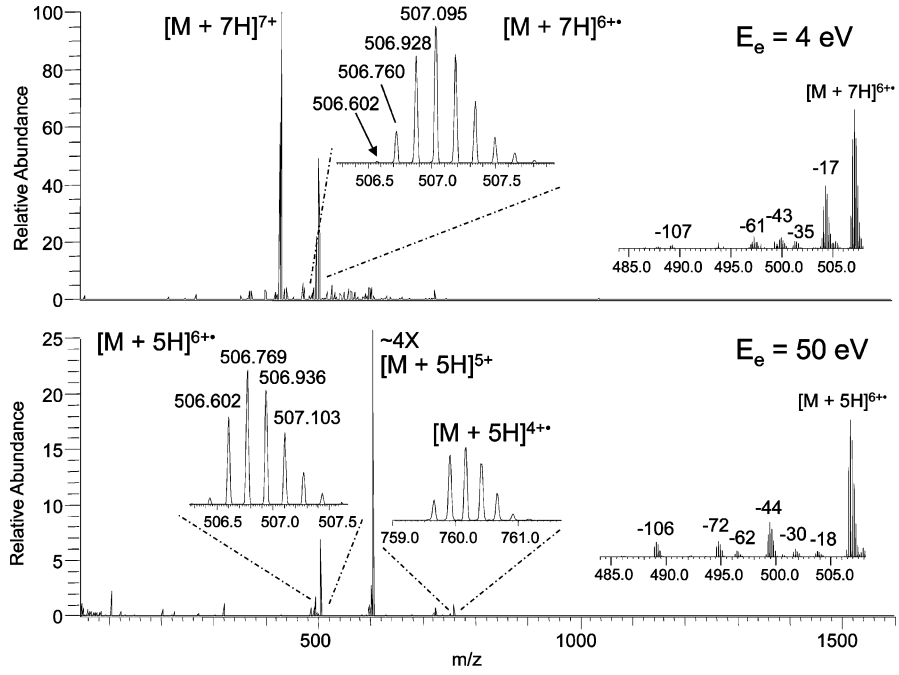

Figure 3. Tandem mass spectra of the peptide DSHAKRHHGYKRKFHEKHHSHRGY. (Top) ECD spectrum of 7+ precursor ions of the peptide: (center inset) isotopic distribution of the reduced species; (right inset) side-chain losses pattern from the reduced species. (Bottom) EID spectrum of 5+ ions of the peptide: (center inset) isotopic distribution of both the ionized and the reduced species; (right inset) side-chain losses pattern from the ionized species.

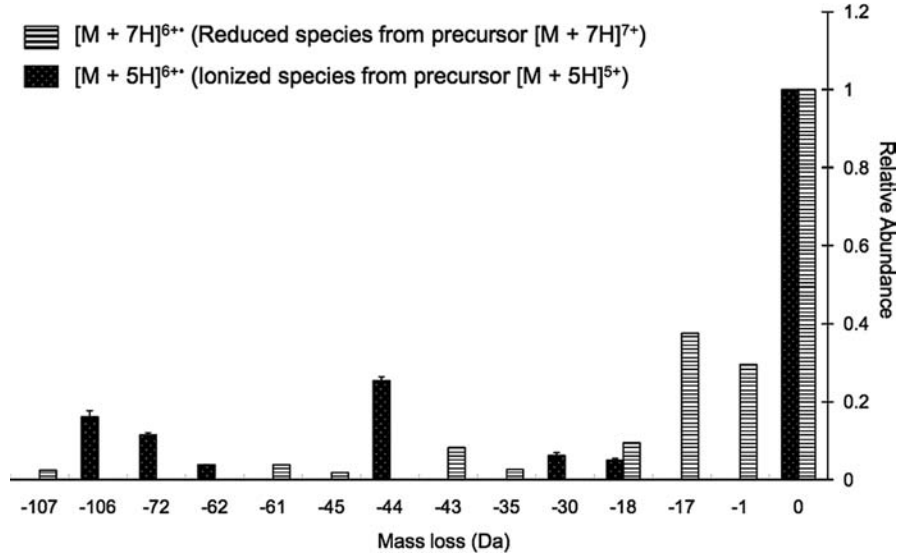

Figure 4. Relative abundance of side-chain losses of peptide DSHAKRHHGYKRKFHEKHHSHRGY: (striped columns) losses from the reduced species of 7+ precursor ions; (solid columns) losses from the ionized species of 5+ precursor ions.

different. The reduced ions in ECD are a hydrogen-surplus species where the number of extra hydrogens exceeds by one the charge state, while the ionized species in EID are hydrogen-deficient ions, with the charge state exceeding by one the number of ionizing protons. As a result of this difference, the masses of the two species differ by the mass of two hydrogen atoms. It appears that the chemical nature of the radicals is the key factor determining the difference in the small loss patterns. The reduced species lost 1, 17, 18, 35, 43, 45, 61, and 107 Da, which are identified as the losses of a hydrogen atom (−1.008 Da), NH_3 (−17.026 Da), H_2O (−18.011 Da), $NH_3 + H_2O$ (−35.037 Da), $^{\bullet}C(NH_2)=NH$ (43.030 Da), $^{\bullet}COOH$ (−44.998 Da), $^{\bullet}C(NH_2)=NH + NH_3$ (−61.040 Da), and $CH_2(C_6H_4O) + H^{\bullet}$ (−107.050 Da). The losses from the ionized species included 18, 30, 44, 62, 72, and 106 Da, identified as losses of H_2O, H_2CO (−30.011 Da), CO_2 (−43.990 Da), $CO_2 + H_2O$ (−62.000 Da), $CH_2CHCOOH$ (−72.021 Da), and $CH_2(C_6H_4O)$ (−106.042 Da). No loss of a radical was identified from the ionized species, while three different radicals were lost from the reduced species. Note also that in at least two cases, 44/45 Da and 106/107 Da losses, more energetic EID demonstrated a 1 Da *smaller* loss than supposedly softer ECD. These differences may be due to the role of the extra hydrogen atom in ECD. This atom can be formed by neutralization of a protonated site, while charge neutralization in EID following double ionization is more likely to quench a hole (radical positive charge), resulting in electronic excitation with subsequent energy conversion to vibrational modes. Indeed, double ionization by >30 eV electrons creates

two holes which, due to their mobility, can move a long distance away from the site of original ionization to minimize the Coulombic repulsion between themselves as well as with other positive charges.[24] The charge migration in polypeptides can be very fast, faster than vibrational energy redistribution. After reaching a certain stable site (e.g., N-terminal amine), the hole can trigger hydrogen atom transfer that converts it into a protonated site and creates a metastable neutral radical elsewhere, for example, at the C-terminus or at aromatic or carboxylic side chains. If now an electron is recaptured by the protonated site, a hydrogen atom can be ejected as a result, like in ECD. Consistent with such a process, a small peak is observed below *m/z* 506.602 in the inset of Figure 3 with the isotopic cluster of the EID oxidized species. This H-loss peak is, however, much smaller than the peak at *m/z* 506.760 corresponding to hydrogen loss from the ECD reduced species. The low abundance of hydrogen loss in EID is not surprising—for it to happen, *both* holes in the doubly ionized species have to convert into protonated sites. Indeed, in ECD the captured electron preferentially neutralizes the site with the highest recombination energy (RE).[25] The same tendency is expected in EID as well, meaning that charge neutralization will preferentially occur at a radical charge site (RE in multiply charged polypeptides >11 eV) and not at a protonated site (RE <7 eV).

Side-chain losses from the reduced species in ECD have been characterized earlier[26,27] and found to be of diagnostic value for the presence of specific amino acids.[28,29] We do not have enough statistics to postulate a strong link between the amino acid content and small losses from oxidized species in EID, but such a link is very likely. For instance, the 106 Da loss is most likely to originate from the tyrosine side chain and 72 Da loss from the glutamic acid side chain. Both Tyr and Glu side chains are easily ionizable by electrons, and can be the sites of electron recapture. The electron recapture process releases as much energy as it takes to remove an electron, that is, >11 eV. Such a large input of energy is likely to cause very fast fragmentation. The fact that the lost species are even-electron neutrals and not radicals as in ECD is consistent with the suggestion that the electron recapture site responsible for these losses is a radical charge (hole) and not a protonated site.

Backbone Fragmentation. Figure 5A presents the average mass of the fragments as a function of the electron energy in the interval ~30−90 eV. The presented data are averaged over three independent experiments. To exclude the influence of small losses and thus to increase the relative weight of backbone fragmentation, ions with masses higher than M − 130 Da were excluded from the top two plots. As expected, the overall trend is that of the fragment mass decrease as the electron energy increases. However, there is a small but significant local maximum around 55−60 eV which is corroborated by other pieces of evidence. The middle section of Figure 5 presents a plot of the average charge state of the fragments. Here again one detects a small but discernible local maximum located approximately at the same energy. Finally, the lower plot that presents the relative abundance of the oxidized species also contains a similar feature. Taken together, these local maxima represent evidence for a specific process occurring around 55−60 eV. This process is in our opinion the double ionization of the molecular ions $[M + nH]^{n+}$ by complete ejection of one electron and incomplete ejection of the other. The incompletely ejected electron (which may have the same spin as the incoming electron and therefore engage in a weaker interaction than in the case of opposite spins) is excited only to a high orbit. The lifetime λ of the formed $[M + nH]^{(n+1)+\bullet *}$ excited species depends upon such factors as the internal energy T_{int} of the ion (higher T_{int} gives shorter λ) as well as the radius r of the excitation orbit (higher r results in longer λ). During the lifetime λ, there are two holes existing in the molecular ion, and this species apparently becomes a diradical $[M + nH]^{(n+2)+\bullet\bullet}$. The two holes, if formed close to each other or to other protonated sites, quickly move to a site with lower ionization energy.[18] The potential energy decrease in such a process is released as vibrational heating. An additional mechanism of energy relaxation is the transfer of a hydrogen atom from an acidic group to the charged radical site, which converts it to a protonated group.[24] Preferentially, this process involves the phenolic hydrogen of Tyr or carboxylic hydrogen from Glu, Asp, or C-terminus, but also backbone amide nitrogens and C_α-hydrogens can be involved. The dehydrogenated groups are prone to lose neutral molecules; for example, $RCOO^\bullet$ rapidly loses CO_2.[21,30] The abundant losses in EID of this and other molecules, as well as a dehydrogenated Tyr side chain, may be evidence of a hydrogen transfer process.

Eventually, the electron excited to a high orbit returns to the ground state. In choosing between the two sites, the electron is likely to elect the one with the highest recomination energy, that is, the radical hole. The energy is released as internal energy, and can cause small losses (or b-/y-ions) from the oxidized species. However, if λ is long enough for both holes to be converted into protonated groups, the two-hole diradical $[M + nH]^{(n+2)+\bullet\bullet}$ becomes $[M^{\bullet\bullet} + (n+2)H]^{(n+2)+}$, where $M^{\bullet\bullet}$ is a neutral diradical. Moreover, the two radicals can in principle recombine, creating the molecule $\mu = M - H_2$ by forming a double bond or an intramolecular link. When the electron lands on this $[\mu + (n+2)H]^{(n+2)+}$ molecular ion, a process similar to ECD occurs. The outcome of this process is also similar to ECD, that is, loss of a hydrogen atom or a small molecule from the reduced species $[\mu + (n+2)H]^{(n+1)+\bullet}$, or $N-C_\alpha$ bond cleavage (c-/z-type ions).

If hydrogen rearrangement process occurs, it should leave a signature. Upon the double-bond formation in μ, at least a fraction of the observed c-/z-ions should contain two hydrogen atoms less than the usual c-/z-ions of M. We have found such ions in the EID mass spectra. The region with c_{10}^{2+} ions is enlarged and shown in Figure 2. The theoretical *m/z* of $c_{10}^{2+\prime}$ ions is 608.8511, and thus the peak observed at *m/z* 608.827 most likely corresponds to consecutive side-chain losses from both leucine and methioine (theoretical *m/z* 608.8269). There is an ion ca. 2 Da lighter at *m/z* 607.844, which is only 1.2 ppm away from the theoretical value of 607.8433 for H_2 loss from $c_{10}^{2+\prime}$ ions.

EID of Folded Proteins. One of the important EID features is the large amount of energy deposited in the precursor ion

(24) Nielsen, M. L.; Budnik, B. A.; Haselmann, K. F.; Olsen, J. V.; Zubarev, R. A. *Chem. Phys. Lett.* **2000**, *330*, 558–562.
(25) Kjeldsen, F.; Savitski, M. M.; Adams, C. M.; Zubarev, R. A. *Int. J. Mass Spectrom.* **2006**, *252*, 204–212.
(26) Cooper, H. J.; Hudgins, R. R.; Hakansson, K.; Marshall, A. G. *J. Am. Soc. Mass Spectrom.* **2002**, *13*, 241–249.
(27) Fung, Y. M. E.; Chan, T. W. D. *J. Am. Soc. Mass Spectrom.* **2005**, *16*, 1523–1535.
(28) Haselmann, K. F.; Budnik, B. A.; Kjeldsen, F.; Polfer, N. C.; Zubarev, R. A. *Eur. J. Mass Spectrom.* **2002**, *8*, 461–469.
(29) Fälth, M.; Savitski, M. M.; Nielsen, M. L.; Kjeldsen, F.; Andren, P. E.; Zubarev, R. A. *Anal. Chem.* **2008**, *80*, 8089–8094.
(30) Kjeldsen, F.; Silivra, O. A.; Zubarev, R. A. *Chem.—Eur. J.* **2006**, *12*, 7920–7928.

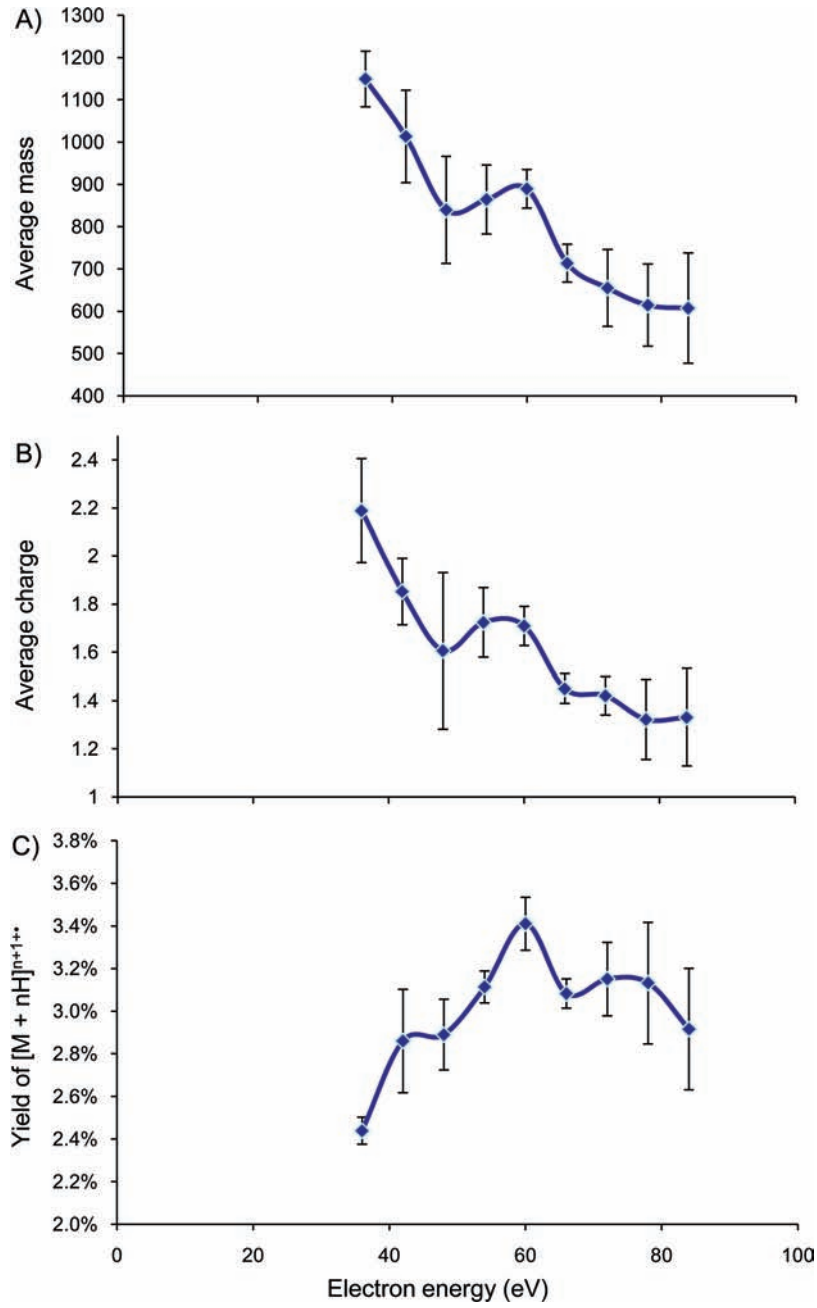

Figure 5. EID results on 6+ ions of peptide DSHAKRHHGYKRKFHEKHHSHRGY against the electron energy used: (A) average mass of fragment ions; (B) average charge state of fragment ions; (C) yield of ionized species.

before fragmentation. The excess of this energy is converted into vibrational degrees of freedom. As a consequence, folded proteins that are relatively stable in the gas phase fragment much more readily, as in "plasma ECD".[31] Figure 6 shows in comparison ECD and EID mass spectra of dications of Trp cage protein. While ECD produces just five backbone fragments, large z-ions,[32,33] EID gives a whole range of fragments with 100% sequence coverage. Notably, c-ion series appears only at energies exceeding 25 eV. This is not surprising, given the tight conformation of Trp cage dications in the gas phase.[33]

Ubiquitin 7+ ions are also tightly folded in the gas phase.[10] Figure 7 presents its EID mass spectrum, rich in backbone fragments of a, b, c, x, y, and z types. Among these ions, there are several pairs of complementary fragments. Their summed charge, calculated as charge state average weighted by the fragment abundances in the respective charge states, reveals the charge state of the transient ionic species that gave rise to these fragments (histogram in Figure 8). For instance, in collisional dissociation such a sum is usually equal to $n+$, that is, the charge state of the precursor ions, while in ECD it is close to $(n-1)+$, which reflects the charge of the fragmenting in ECD transient species $[M + nH]^{(n-1)+\bullet}$. In EID of 7+ precursors, the majority of (c, z) complementary ion pairs gave the total of seven, consistent with single ionization followed by electron capture as the dominant process. At the same time, there is a smaller

(31) Sze, S. K.; Ge, Y.; Oh, H. B.; McLafferty, F. W. *Anal. Chem.* **2003**, *75*, 1599–1603.
(32) Adams, C. M.; Kjeldsen, F.; Zubarev, R. A.; Budnik, B. A.; Haselmann, K. F. *J. Am. Soc. Mass Spectrom.* **2004**, *15*, 1087–1098.
(33) Patriksson, A.; Adams, C.; Kjeldsen, F.; Raber, J.; van der Spoel, D.; Zubarev, R. A. *Int. J. Mass Spectrom.* **2006**, *248*, 124–135.

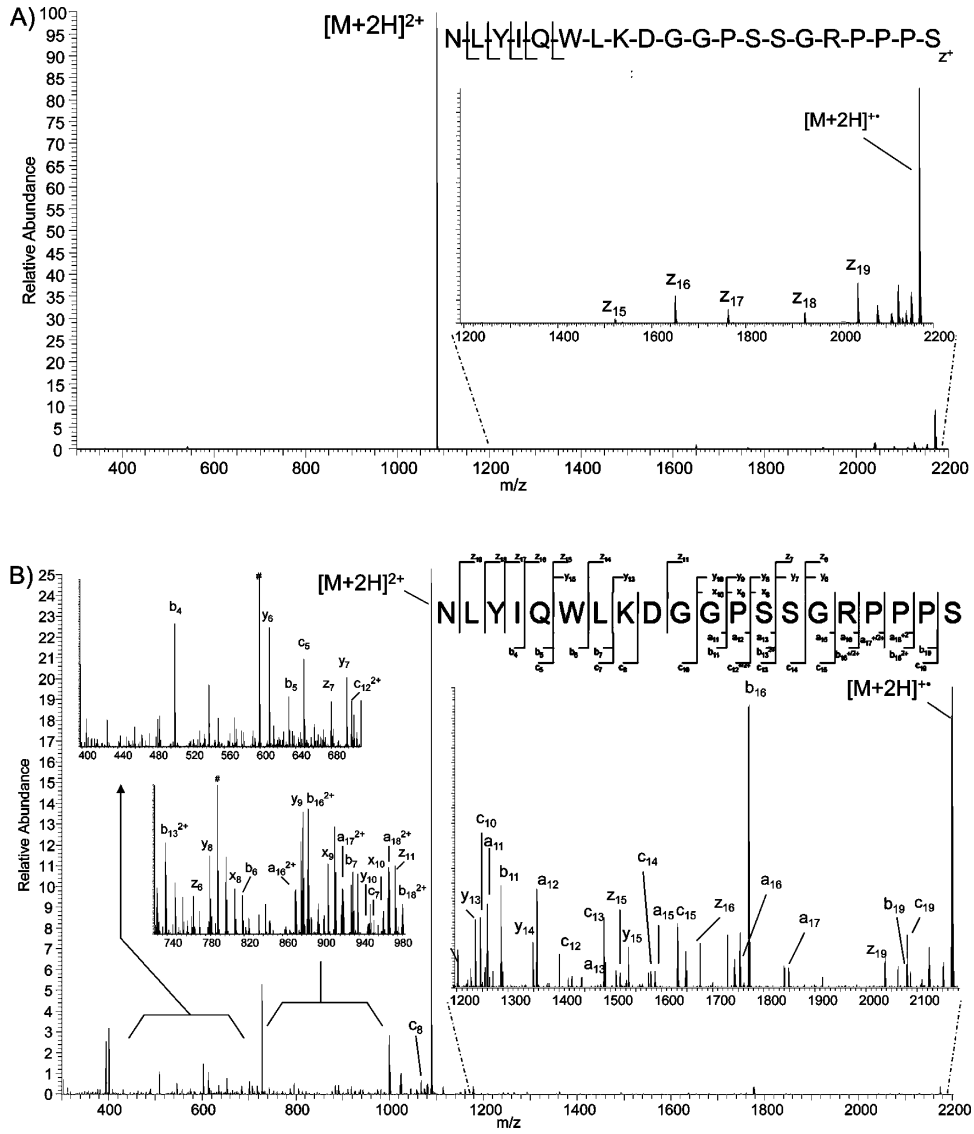

Figure 6. (A) ECD and (B) EID mass spectra of the 20-mer polypeptide Trp cage.

group of (c, z) pairs with even higher average charge state, up to 8+, consistent with N−C_α bond cleavage following double ionization to 9+ with subsequent electron capture. The (a, x) complementary ion pairs show a positive shift in average charge state compared to the majority of (c, z) pairs: their average charges add up preferentially to 8+ (note that because charge averaging was involved, the charge values in Figure 8 do not have to be integers). This shift is consistent with double ionization followed by electron capture as the dominant process in formation of these species. These results prove that those ions are not HECD products (whose charges would add up to 6) and that double ionization indeed plays a role in EID. Also supportive of this conclusion is the fact that doubly ionized $[M + 7H]^{9+}$ species are very abundant in Figure 7 (see inset).

There is a parallel between the EID process and electronic excitation of ions in the "classical" electron ionization of neutral molecules. The abundant fragmentation in EI is not generally ascribed to double ionization of a neutral molecule with recapture of one electron, although for all organic molecules the electron energy in EI, 70 eV, is above the threshold for double ionization. The reason why we invoke double ionization followed by electron capture as one of the processes in EID (but by no means the only process) is to draw a parallel with ECD, where the fragmenting species are hydrogen-abundant radical cations as opposed to hydrogen-deficient species in EI.[34] This difference in the nature of fragmenting species accounts for the vast difference in the fragmentation mechanisms in these two techniques. In our view, without invoking the ECD-like mechanism it is difficult to explain all fragmentation phenomena observed in EID.

EID Efficiency. Obtaining good EID results with standard FT ICR equipment was not an easy task, but it was possible to measure reproducibly the EID efficiency. The efficiency measures differ in the literature. As the most relevant for our case, we have chosen the ratio between the total charge of the ionic products and the reduction (depletion) of the precursor ion population. This measure takes into account only precursor ions that did change their mass or charge state as a result of interactions with electrons, and it neglects unreacted species. The following values were obtained for singly charged substance P precursor: at electron energy ≈40 eV, 127% ± 5%, at electron energy ≈50 eV, 79% ± 1%, and at electron energy ≈60 eV,

(34) Zubarev, R. A. *Mass Spectrom. Rev.* **2003**, *22*, 57–77.

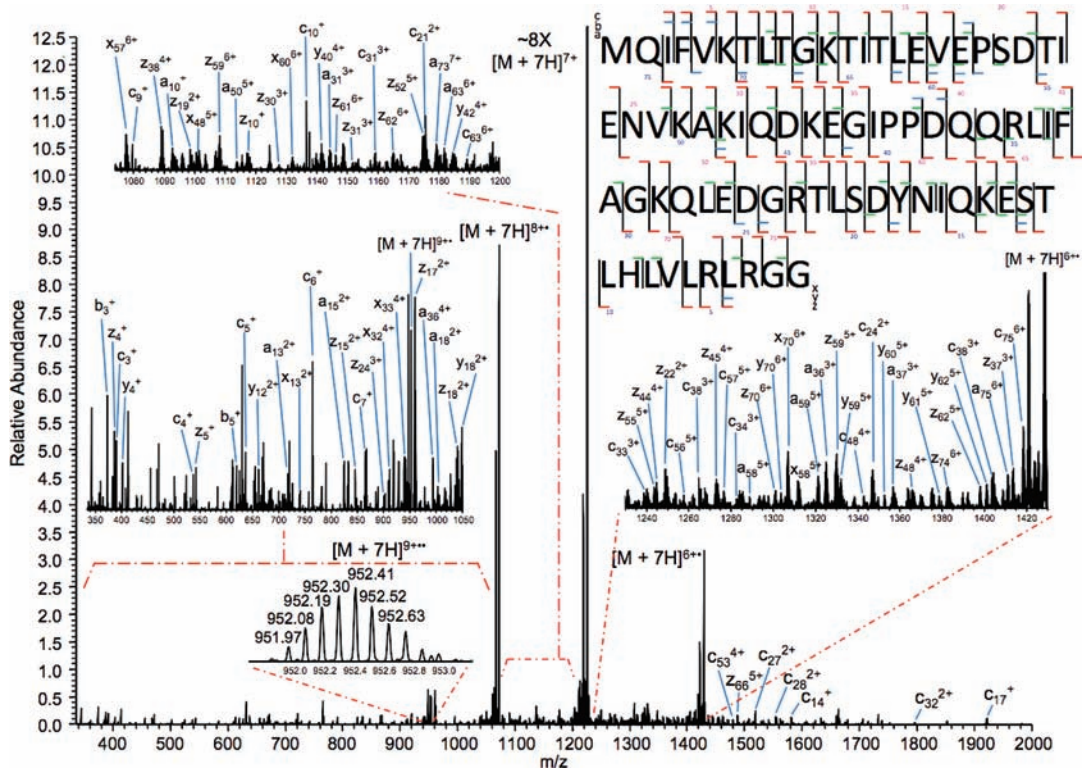

Figure 7. EID mass spectrum of ubiquitin 7+ ions.

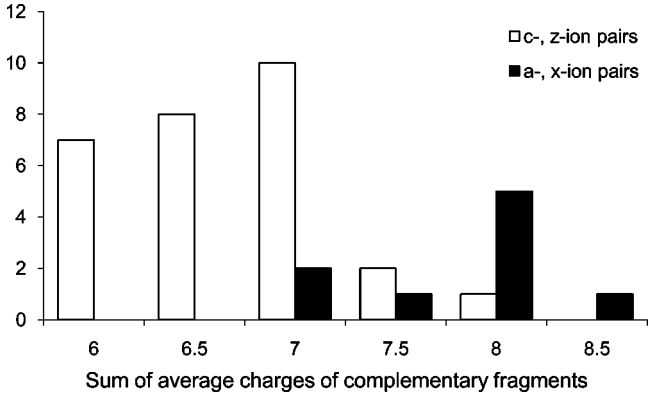

Figure 8. Sum of average charges of complementary fragments in EID of ubiquitin $[M + 7H]^+$ ions. Open columns represent (c, z) ion pairs and solid columns represent (a, x) ion pairs.

65% ± 1%. Thus the theoretical possibility of obtaining >100% efficiency in EID has been confirmed experimentally. The >100% efficiency became possible due to the progression of EID through intermediates in a higher charge state than the precursor ions. This charge-increasing progression is in stark contrast to ECD, where fragmenting intermediates are charge-reduced species.

Besides the EID efficiency, which can be very high, a parameter also relevant for applications is the EID backbone fragment yield, which places the signal of the entire precursor ion population in the denominator and the signal of the EID backbone products in the numerator. Since the undissociated electron ionization products can represent a significant fraction of the EID yield, the EID backbone fragment yield is nowhere near the EID efficiency and in current implementation reaches values of 1−5%. The main limitation seems to be the trapping ability of the Penning trap, which is particularly small in the direction of electron propagation. Implementation of an optimized ICR cell, a special-purpose trap, or an efficient ion cooling method should increase the trapping capacity and improve the EID yield. Another potential is the additional excitation of undissociated electron ionization products, which should lead to their efficient fragmentation.

Conclusion

The new tandem mass spectrometry technique electron ionization dissociation (EID) shows promising results in terms of peptide backbone fragmentation that in many cases produces results similar to ECD. But unlike ECD, EID is applicable to singly charged peptides and proteins in low charge states, and its efficiency, calculated as a ratio of the product charge and the charge of the depleted precursors, can exceed 100%. These features make EID unique among fragmentation methods. The evidence is obtained that EID involve double ionization followed by capture of one of the ejected electrons, with a rearrangement of the oxidized (ionized) species in between these two stages. These are, however, early results; more research is needed for determination of the mechanism and analytical abilities of EID. The ability of EID to provide important backbone fragments can be further improved if higher trapping efficiency is achieved and an ion cooling technique is employed before ion detection.

Acknowledgment. This work was supported by the Swedish Research Council (Grant 621-2007-4410). ThermoFisher Scientific is gratefully acknowledged for technical consultations during EID realization.

JA8087407